

ACTIVATABLE SMART PROBES FOR MOLECULAR OPTICAL IMAGING AND THERAPY

JONATHAN F. LOVELL* and GANG ZHENG*^{†,‡}

**Institute of Biomaterials and Biomedical Engineering and*

†Department of Medical Biophysics, University of Toronto

*‡Division of Biophysics and Bioimaging, Ontario Cancer Institute
Toronto, Ontario M5G 1L7, Canada*

Recent years have seen the design and implementation of many optical activatable smart probes. These probes are activatable because they change their optical properties and are smart because they can identify specific targets. This broad class of detection agents has allowed previously unperformed visualizations, facilitating the study of diverse biomolecules including enzymes, nucleic acids, ions and reactive oxygen species. Designed to be robust in an *in vivo* environment, these probes have been used in tissue culture cells and in live small animals. An emerging class of smart probes has been designed to harness the potency of singlet oxygen generating photosensitizers. Combining the discrimination of activatable agents with the toxicity of photosensitizers represents a new and powerful approach to disease treatment. This review highlights some applications of activatable smart probes with a focus on developments of the past decade.

Keywords: Optical imaging; photodynamic therapy; activatable imaging probes.

1. Introduction

An activatable optical imaging agent must undergo a change in properties so that different states of the probe can be detected and be spatially resolved. The probes generally produce signals based on fluorescence properties, but some produce phosphorescence or luminescence based signals. Measuring an increase in probe emission intensity is a common measurement parameter, although other useful metrics can include decrease in emission intensity, change in excitation or emission wavelength, change in fluorescence lifetime, and also change in emission or excitation ratio when the optical agent is composed of a Förster resonance energy transfer (FRET) pair. The nature of the changes for activatable smart probes may or may not be reversible.

Activatable imaging agents and targeted imaging agents rely on different mechanisms to identify targets of interest. Activatable agents can be localized non-specifically, since their detection is based on a change in optical properties brought about by the target. Targeted agents, on the other hand, migrate to the target of interest. An advantage of activatable probes is that probe signal to noise ratio is

not limited by targeting efficiency. Targeted agents often find their target through passive accumulation in damaged vasculature of tumours, or through the use of antibodies. The high affinity of antibodies for their antigens is the basis for the high resolution and contrast of immunofluorescence microscopy. However, for *in vivo* imaging, antibodies are often limited to extracellular protein targets since their large size does not permit entry across the cell membrane. Targeted imaging agents that do not target correctly create misleading and inaccurate results. In theory, both targeted probe and activated probe mechanisms can be combined to create sensors that display an extremely high level of target specificity. For example, certain peptide constructs can be internalized by cells upon cleavage by specific proteases (Jiang *et al.*, 2004). Modification of such a peptide to incorporate a fluorophore and quencher in the correct arrangement would lead to both the internalization (targeting) and dequenching (activation) of the probe upon interaction with the targeted protease.

Generally, activatable smart probes are not well suited for the non-optical imaging modalities of ultrasound, CT, PET and MRI. Since non-optical techniques rely on probe properties such as acoustic density, electron density, positron density, or ability to cause water relaxation, the signal generated by non-optical probes does not readily change intensity on a molecular level. A good introduction to the characteristics of the various imaging modalities with respect to molecular imaging is available elsewhere (Massoud and Gambhir, 2003). There have been some successful efforts to develop activatable MRI contrast agents using molecules that change water relaxation properties upon enzymatic cleavage, but more work is required to expand that field of research (Meade *et al.*, 2003). Thus, to achieve contrast, non-optical modalities usually rely on the targeting rather than the activation of imaging agents.

2. Optical Imaging Methods

Activatable smart probes have greatly benefitted from advances in imaging technology. The resolution of fluorescence microscopy has continued to improve so that it is now possible to optically distinguish individual fluorophores using single molecule imaging (Moerner, 2007). This sensitivity makes it possible to use activatable smart probes to precisely examine the subcellular localization of the activating target. However, there are still challenges in monitoring the precise activation pattern of optical probes since the probes may diffuse quickly throughout the cell. Activatable probes are better suited to monitor changes that occur within whole cells over time. They also hold much potential for *in vivo* imaging, since probes can be activated by groups of similar cells or areas in the body that contain a higher concentration of a target molecule.

A major limitation of *in vivo* optical imaging in tissue is the shallow penetration of light due to absorbance and scattering in body tissue. By using probes that operate in the near infrared (NIR) region of the light spectra, spanning from

600 nm to 1000 nm, water absorbance in the far infrared and light scattering and autofluorescence in the shorter wavelength range are minimized (Richards-Kortum and Sevick-Muraca, 1996). Using an NIR imaging system, the Weissleder group has pioneered *in vivo* imaging in mice using smart probes that are activated by tumour proteases (Mahmood *et al.*, 1999). Since then, many other targets have been visualized in living organisms using activatable probes. Due to the greater depth of tissue that must be penetrated, optical imaging in humans is still a challenge and may never reach the resolution and depth possible with other imaging modalities. Nevertheless, innovative and refined imaging techniques will improve optical *in vivo* imaging. One advance in imaging technology is the use of multiphoton excitation. Multiphoton excitation permits light of a longer wavelength to be used to excite fluorophores. The phenomenon is well explained elsewhere (Zipfel *et al.*, 2003). Multiphoton excitation is relevant for *in vivo* imaging, where longer wavelength light can more effectively penetrate tissues. Fluorescence lifetime imaging microscopy (FLIM) has been developed and offers the advantage over conventional microscopy of being able to perform measurements that are independent of fluorophore concentration. Since FLIM can measure changes in lifetimes brought about by environmental or chemical change, the probes used in certain FLIM experiments can be considered activatable probes. FLIM has been used to measure the change in the endogenous probe NADH in tissue culture (Ramanujan *et al.*, 2005) and *in vivo* (Skala *et al.*, 2007). New imaging technologies have been combined to create hybrid imaging techniques such as multiphoton FLIM (Peter and Ameer-Bet, 2004).

A promising new approach to fluorescence imaging *in vivo* has come through the development and commercial availability of fluorescence tomography (Ntziachristos *et al.*, 2002). This technology permits the three dimensional reconstruction of fluorescence distribution. Mice are small enough to be completely imaged using this technique. Fluorescence diffuse optical tomography is a related technique that been used to image breast tumours in humans (Ntziachristos *et al.*, 2000). Furthermore, three dimensional tomography based on fluorescence lifetimes has also been developed (Godavarty *et al.*, 2005). As these new and informative three dimensional imaging techniques are further developed and refined, the usefulness of activatable probes will increase.

3. Mechanism of Activation

There are various routes in which different optical activatable smart probes may be activated. The nature of the activation depends on the characteristics of the optically active component of the probe, as well as the overall probe design. Figure 1 shows some common activation routes that lead to a change in the optical properties of probes. Figure 1A shows the design of a typical probe for sensing protease activity. A fluorophore is linked to a quenching moiety by a peptide linker. The amino acid sequence of the peptide linker is recognized by a specific proteolytic enzyme or enzyme class. Upon linker cleavage by the enzyme, the fluorophore and quencher

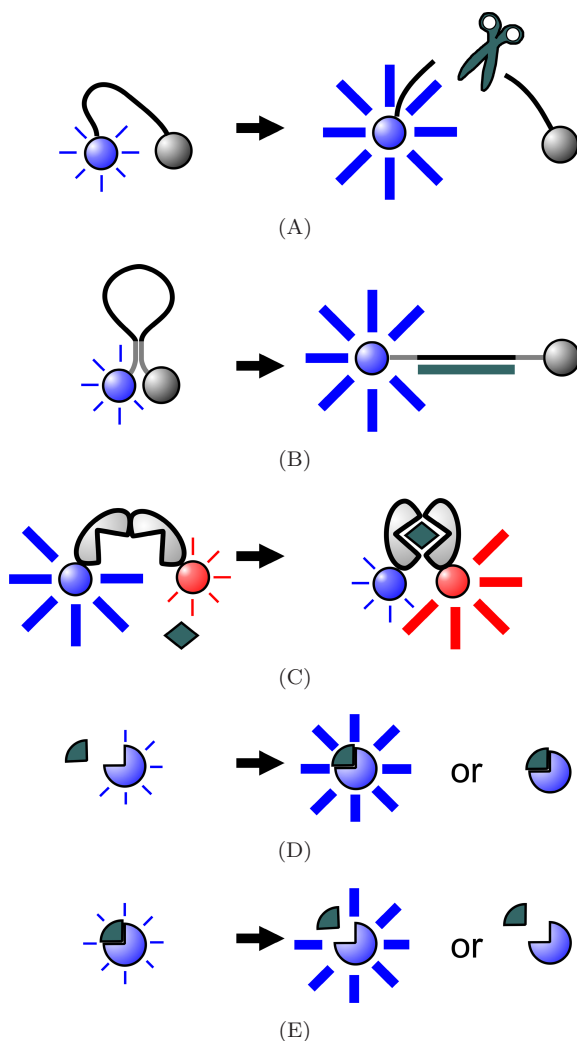


Fig. 1. Numerous activation pathways exist for activable smart probes. See text for explanation.

disassociate, which leads to dequenching and brighter emission. Figure 1B shows the design of a standard beacon for sensing nucleic acids. The linker in this case is a nucleic acid hairpin loop structure. The hairpin portion of the beacon, which consists of about 4 to 6 hybridizing base pairs, physically forces the fluorophore and the quencher together. When a target nucleic acid hybridizes with the loop portion, the hairpin portion of the beacon comes apart and the quencher and fluorophore move apart, resulting in decreased quenching efficiency and greater fluorescence signal.

Figure 1C shows the design of a genetically encoded FRET sensor. This versatile construct consists of two fluorescent proteins, usually CFP and YFP variants,

connected by a linker protein. The genetically encoded linker protein can be a protein that changes conformation upon a substrate binding. Upon conformational change in the linker protein, the positioning of the two FRET proteins changes and results in a change in the FRET efficiency. Figures 1D and 1E represent smaller activatable smart probes that are not composed of amino acid or nucleobase subunits. Figure 1D shows an activatable optical probe that becomes brighter or dimmer upon binding or interacting with a specific substrate. This change can stem from either a substrate enhancement or quenching of the probe emission through contact with the fluorophore. In contrast, Figure 1E shows an activatable optical probe that becomes brighter or dimmer after the removal of part of the fluorophore by the target.

3.1. Enzyme activated optical probes

Because of their abundance, diversity and catalytic activity, enzymes are major targets for activatable smart probes. Proteases, which are involved in many biochemical processes, have been a central focus. One of the first protease activatable imaging agents was developed for the Factor Xa protease by fusing two FRET capable GFP variants linked with a Factor Xa peptide substrate (Mitra *et al.*, 1996). The cleavage of the peptide linker between the two fluorescent proteins causes their dissociation and subsequent loss of FRET. A similar approach of using two fluorescent proteins fused by a specific linker sequence has been applied to detect other proteases including Botulinum toxin (Dong *et al.*, 2004), caspases (Lin *et al.*, 2006), secretases (Lu *et al.*, 2007), and matrix metalloproteases (Zhang *et al.*, 2008). Some activatable optical probes rely on a conformational change, rather than cleavage, of the linker protein. The conformational change brought about by substrate binding alters the position of the two flanking fluorescent proteins which results in a change in FRET (Figure 1C). By using a protein linker consisting of both a specific phosphorylation substrate and a phosphorylation binding protein, enzymatic substrate phosphorylation and subsequent binding results in a conformational change, which moves the tethered fluorescent proteins closer together and results in higher FRET efficiency (Zhang *et al.*, 2001).

Genetically encoded enzyme sensors have limitations that can be circumvented by using chemically synthesized probes. Genetically encoded sensors display a relatively low change in signal. Typically, the ratio of donor to acceptor emission changes less than two fold, which is a smaller change than most chemically synthesized activatable probes. A second drawback is that genetic probes will not likely be used for human imaging or therapy since this would involve the challenging task of transfecting humans with engineered genes.

A multitude of synthetic activatable enzyme sensing probes have been developed in the past decade. Many have been tested successfully in live mice, showing their potential for eventual use in human diagnostics and therapy. One of the first instances of imaging enzyme activity *in vivo* used a synthetic activatable optical

probe that detected tumour associated proteases in mice (Weissleder *et al.*, 1999). This study used a polymer based self quenching infrared probe that, upon cleavage by lysine specific proteases, displays a 12 fold increase in emission. As detailed in their review, the Weissleder group has continued to expand this technique, and using similar methodology, has imaged enzyme activity *in vivo* for proteases associated with a variety of ailments including cardiovascular disease, cancer and HIV (Funovics *et al.*, 2003). Recently, these activatable smart probes have been validated ex-vivo in deceased humans suffering from carotid endarterectomy, where cathepsin protease activity was detected (Jaffer *et al.*, 2007). Protease activity *in vivo* has also been visualized using peptides linked to a large dendrimer core (McIntyre *et al.*, 2004), as well as smaller non polymeric molecules (Blum *et al.*, 2007). Extracellular proteases are good targets for activatable probes since the beacon does not require cellular uptake and often tumour vasculature permits beacon accumulation and subsequent activation. While most enzyme sensing activatable optical probes have focused on proteases, others have been developed for a range of different enzyme targets. Two probes have been designed for imaging beta-galactosidase activity *in vivo* (Tung *et al.*, 2004; Wehrman *et al.*, 2006). This enzyme is often used during in genetic engineering and such a probe could facilitate identification of successfully modified cells. Another enzyme often used in genetic engineering, beta-lactamase, has also been the target for an infrared activatable probe that has been validated in cells (Xing *et al.*, 2005). By designing an activatable probe with an ester linkage, esterase activity has been imaged in tissue culture (Kim *et al.*, 2007). Lipase is another enzyme that has been examined using activatable optical probes. By using modified fluorescent lipids that are dequenched after lipase cleavage, lipid processing in the digestive system was visualized in live zebra fish (Farber *et al.*, 2001).

3.2. Nucleic acid activated probes

Nucleic acid detection and imaging in living cells using molecular beacons was developed over a decade ago (Tyagi and Kramer, 1996). Molecular beacons have received considerable attention and are reviewed in deeper detail elsewhere (Goel *et al.*, 2004, Tan *et al.*, 2004). A molecular beacon is generally a self folding nucleic acid construct between 20 and 30 bases long, which holds together a fluorophore and a quencher on the extreme ends by 4 to 6 matching bases (Figure 1B). When the central loop region, designed to be complimentary to a target nucleic acid, hybridizes to the target, the beacon unfolds and the separation of the fluorophore and quencher leads to dequenching and stronger fluorescence emission.

Molecular beacons have emerged as a tool to determine the distribution and movement of RNA in living cells. Molecular beacons were used to visualize mRNA movement of developmental mRNAs, highlighting the importance of mRNA distribution in oocytes (Bratu *et al.*, 2003). Molecular beacons have also been used to visualize mRNA transport into the nucleus, (Vargas *et al.*, 2005) and viral mRNA behaviour of the poliovirus (Cui *et al.*, 2005). Since measurement of RNA expression

levels does not require imaging, molecular beacons have not seen an increase in usage comparable to reverse transcriptase Polymerase Chain Reaction (PCR) and genetic microarrays. However, due to their utility at sensing specific nucleic acids, molecular beacons are sometimes used in real time PCR to monitor the amplification of target genes.

Many new reports about molecular beacons describe implementations of new beacon designs. Modified bases, especially 2-O-methyl bases, are used to encourage better hybridization (Molenaar *et al.*, 2002) and to prevent beacon degradation (Bratu *et al.*, 2003). Peptide nucleic acid (PNA) has also successfully been used to construct beacons that can image cellular RNA and offer improved signal to noise and hybridization properties (Xi *et al.*, 2003). Several modifications of overall probe design have also been reported. Dual FRET beacons use two sets of molecular beacons that hybridize to neighbouring RNA sections and generate a FRET based signal (Santangelo *et al.*, 2004). Quenched auto ligating (QUAL) probes function in a similar manner in the sense that two probes hybridize to one contiguous target RNA section. One of the probes then catalyzes the cleavage of the quenching group on the other self quenched probe, resulting in higher emission (Sando *et al.*, 2004).

The use of molecular beacons for *in vivo* imaging represents an intriguing possibility to image RNA expression in an entire organism, although the challenge of delivery of the beacons must be overcome first.

3.3. Ion activated probes

Ion activated probes are by far the most commonly used activatable imaging agents. This is mainly due to the efficiency and importance of calcium imaging. Activatable optical probes have been designed and validated for a wide range of other ions as well, including zinc, iron and hydrogen ions.

The report which describes the creation of the Fluo dyes, which increase fluorescence emission in the presence of calcium, has become the second most highly cited publication in the Journal for Biological Chemistry (Grynkiewicz *et al.*, 1985). Upon binding calcium, these probes display a wavelength shift and an approximate 30 fold increase in emission intensity. These and other classical ion sensing probes, many which have been used for decades, have been thoroughly reviewed elsewhere (Johnson, 1998). Calcium detection has also been examined using a genetically encoded activatable probe. The Cameleon sensor uses a FRET donor CFP linked to a FRET acceptor YFP by calmodulin, a calcium binding protein (Miyawaki *et al.*, 1997). Subsequent work has improved the properties of Cameleon so that it displays a better dynamic range in physiological calcium concentrations (Truong *et al.*, 2001). Upon binding calcium, the sensor undergoes a conformational change and increases the FRET emission ratio approximately 2 fold. Cameleons have been used in transgenic drosophila larvae (Liu *et al.*, 2003) as well as transgenic mice (Hara *et al.*, 2004) to measure neuron activity and calcium distribution. Another genetically encoded ion sensor is the hydrogen ion sensing pHluorin protein (Miesenbock

et al., 1998). This GFP mutant displays a three fold range in the ratio of two excitation peaks as the pH shifts from 5 to 8. Fluorescence proteins and how they can be used effectively have been the subject of many good reviews (Giepmans *et al.*, 2006, Chudakov *et al.*, 2005, Roessel and Brand, 2001).

Recent research has led to the creation of new small molecule smart probes that can visualize ions. An activatable fluorescent probe, FluoZin3, has been developed for sensing zinc, which is involved in neuron function (Gee *et al.*, 2002). FluoZin3 has a high affinity for zinc and increases emission upon zinc binding 100 fold. This probe is currently restricted to imaging extracellular zinc, and has been used to examine zinc regulation in rat brain slices (Kay, 2003). A chelatable iron specific probe was developed which fuses an iron chelating agent with a rhodamine dye, resulting in the fluorophore quenching upon iron binding (Petrat *et al.*, 2002). A copper specific sensor was developed and validated that displays a 5 fold increase in emission detection when exposed to copper (Yang *et al.*, 2005). Chemists have synthesized probes for a variety of other ions including chloride (Bai *et al.*, 2005) and lead (Kwon *et al.*, 2005), although these probes have not yet been validated in cells.

3.4. Reactive oxygen species (ROS) activated probes

Activatable smart probes that can detect ROS have seen a much new progress. Due to the intrinsic reactivity of ROS, many probes are based on a change in fluorescence properties upon ROS induced chemical modification. The singlet oxygen sensor DanePy is oxidized upon exposure to singlet oxygen and becomes less fluorescent (Hideg *et al.*, 2002). This probe has been used to visualize singlet oxygen production in leaves after stress. Another fluorescent probe, Singlet Oxygen Sensor Green has also been developed and, unlike DanePy, is currently commercially available (Flors *et al.*, 2006). Luminescent probes have also been developed that are suitable for imaging singlet oxygen (Yasui and Sakurai, 2000). Smart probes have been developed for another ROS, hydrogen peroxide, which is involved in cell signalling. The hydrogen peroxide sensing probes show good specificity since they show little response to other ROS. One reported probe is based on linking a fluorophore with a cleavable boron linkage (Miller *et al.*, 2007), while another is based on peroxalate ester luminescent nanoparticles (Lee *et al.*, 2007). Upon interaction with hydrogen peroxide, the linker is cleaved and the probe is unquenched. A genetic technique for an activatable ROS sensor has been developed by fusing a FRET pair of proteins linked by a hydrogen peroxide sensing protein (Belousev *et al.*, 2006). Another important signalling radical, nitric oxide, is the target of an activatable probe capable of a 20 fold increase in emission (Kojima *et al.*, 1998). Oxygen monitoring probes have also been developed and validated recently. A phosphorescence based sensor that is quenched by oxygen has been used to image oxygen in rats (Dunphy *et al.*, 2002). A fluorescence based oxygen sensing smart probe has also been developed to image intracellular oxygen as well (O'Riordan *et al.*, 2007). Both these oxygen sensing probes displayed a 5 fold signal difference upon activation.

3.5. Activatable optical probes for therapy

While activatable smart probes usually incorporate a fluorophore, it is possible to replace the fluorophore with a photosensitizing agent, creating a photodynamic beacon. This approach was first shown using the photosensitizer pyropheophorbide and a peptide linker specific for caspase 3 attached to a carotenoid quencher (Chen *et al.*, 2004). Unlike conventional fluorophores, photosensitizers generate singlet oxygen upon excitation by light. *In vivo*, singlet oxygen goes on to attack many cellular targets, leading to apoptotic cell death (Oleinick and Evans, 1998). Photosensitizers are the basis of photodynamic therapy (PDT), a form of cancer treatment that has been in use for decades. A photosensitizer behaves similarly to a fluorophore in the sense that it can be excited with visible or NIR light, and its signal can be attenuated by a quencher. Upon activation, photodynamic smart probes therefore become toxic to cells. Photosensitizers not only generate singlet oxygen, but often also generate fluorescence emission. The fluorescence lifetime distribution of photosensitizers has been examined in cells using FLIM (Russell *et al.*, 2007). Furthermore, the fluorescence of photosensitizers can be used to monitor singlet oxygen generation for photodynamic beacons (Stefflova *et al.*, *Frontiers in Bioscience*, 2007). A PDT based activatable probe has been developed that becomes toxic to tumour cells that express the matrix metalloprotease 7 enzyme (Zheng *et al.*, 2007). This protease is overexpressed in certain tumours. Tumours implanted in the mice showed tumour shrinkage when treated with the probe and light.

Photosensitizing agents have also been used to create molecular beacons that kill cells based on the expression of specific RNA targets using molecular beacon type constructs (Chen *et al.*, 2008, *in press*). This represents a powerful therapeutic technique that could be widely adaptable to a variety of diseases by simply changing the target mRNA.

Combining activatable optical probes with PDT represents a new and novel therapeutic technique that has the potential to realize previously unachievable layer of specificity to disease treatment. The potential of photodynamic molecular beacons for cancer imaging and therapy has been examined by our group previously (Stefflova *et al.*, *Curr Med Chem*, 2007).

3.6. Other noteworthy activatable smart probes

While many activatable sensors are specific for detecting enzymes, nucleic acids, ions or ROS, there are probes that can detect many other targets, including peptides, carbohydrates, lipids, and protein behaviour. A probe that can detect amyloid plaques has been developed that displays a 400 fold increase upon binding amyloid. It has been used to image amyloid plaques in mice brains (Nesterov *et al.*, 2005). Carbohydrate sensing using activatable probes has received a great deal attention, although there has not been success yet in creating a suitable chemical *in vivo* imaging agent (Moschou *et al.*, 2004). Carbohydrate sensing genetically encoded

Table 1. Comparison of selected optical activatable smart probes.

Activator	Probe name	Type	Activatable Signal	Fold change	Em. λ (nm)	Imaging host	Ref
Amyloid fibre	NIAD-4	C	Em. increase	400	610	Transgenic mouse brain slices	Nesterov <i>et al.</i> , 2005
Beta-galactosidase	DDAOG	C	Em. increase	3	660	Mouse	Tung <i>et al.</i> , 2004
Beta-galactosidase and luciferase	A caged luciferin beta-galactoside reporter	C	Chemiluminescence increase	200	—	Mouse	Wehrman <i>et al.</i> , 2006
Beta-lactamase	CNIR3	C	Em. increase	10	660	C6 cells	Xing <i>et al.</i> , 2005
Botulinum neurotoxin	Botulinum toxin FRET sensor	G	Change in em. ratio	1.25	470/530	PC12 cells	Dong <i>et al.</i> , 2004
Calcium	Cameleon	G	Change in em. ratio	2	480/530	HeLa cells	Miyawaki <i>et al.</i> , 1997
Caspase-2	CFP-CRS-DsRed	G	Change in em. ratio	1.7	475/580	Hela cells	Lin <i>et al.</i> , 2006
Cathepsins	GB138	C	Em. increase	5	804	Mouse	Blum <i>et al.</i> , 2007
Cathepsin K	Cy5.5 PEG polymer	C	Em. increase	3.5	720	Human (ex-vivo)	Jaffer <i>et al.</i> , 2007
Cu(I)	CTAP-1	C	Em. increase	4.5	490	3T3 cells	Yang <i>et al.</i> , 2005
Esterase	Probe 2	C	Em. increase	5	800	BT-20 cells	Kim <i>et al.</i> , 2007
Fe 2+	RPA	C	Em. decrease	20	600	Rat hepatocytes	Petrat <i>et al.</i> , 2002
GAPDH mRNA	Cy3 – oligo – BH2	C	Em. increase	10	570	MiaPaca-2 cells	Nitin <i>et al.</i> , 2004
Glucose	FLIPglu	G	Change in em. ratio	1.1	485/530	Cos-7 cells	Fehr <i>et al.</i> , 2003
Hydrogen peroxide	HyPer probe	G	Change in exc. ratio	3	516	Cos-7 cells	Belousev <i>et al.</i> , 2006
Hydrogen peroxide	Peroxy Crimson 1	C	Em. increase	40	584	HEK 293 cells	Miller <i>et al.</i> , 2007
Hydrogen Peroxide	Peroxalate nanoparticles	C	Chemiluminescence increase	1.8	460–630	Mouse	Lee <i>et al.</i> , 2007
Inositol 3 Phosphate	LIBRA	G	Change in em. ratio	1.1	480/535	SH-SY5 cells	Tanimura <i>et al.</i> , 2004
Lysine specific proteases	Cy5.5 PEG polymer	C	Em. increase	12	690	Mouse	Weissleder <i>et al.</i> , 1999
Maltose	FLIPmal	G	Change in em. ratio	1.1	485/530	Yeast	Fehr <i>et al.</i> , 2002

Table 1. (Continued)

Activator	Probe name	Type	Activatable Signal	Fold change	Em. λ (nm)	Imaging host	Ref
MMP7	Photodynamic molecular beacon	C	Singlet oxygen and em. increase	12	670	Mouse	Zheng <i>et al.</i> , 2007
MMP7	Fluorescein labeled peptide-dendrimer	C	Em. increase	5	520/570	Mouse	McIntyre <i>et al.</i> , 2004
Nitric Oxide	Diaminofluorescein	C	Em. increase	100	515	Rat Muscle cells	Kojima <i>et al.</i> , 1998
Oxygen	Oxyphor G2	C	Phosphorescence τ decrease	5	790	Rat	Dunphy <i>et al.</i> , 2002
Oxygen	PdCfPK	C	Phosphorescence em. decrease	4.5	796	Hela cells	O'Riordan <i>et al.</i> , 2007
pH	pHluorin	G	Change in exc. ratio	2.5	510	Hela cells	Miesenbock <i>et al.</i> , 1998
Phospholipase A	PED6	C	Em. increase	5	515/570	Zebrafish	Farber <i>et al.</i> , 2001
Single nucleotide polymorphisms	QUAL probe	C	Em. increase	7	520/580	E. Coli	Sando <i>et al.</i> , 2003
Singlet oxygen	DanePy	C	Em. decrease	3	550	Spinach leaves	Hideg <i>et al.</i> , 2002
Tyrosine kinase	Tyrosine kinase FRET sensor	G	Change in em. ratio	1.35	475/530	B82 and MEF cells	Ting <i>et al.</i> , 2001
vav oncogene	EDANS -oligo Dabcyl	C	Em. increase	15	490	TKts13 and K562 cells	Sokol <i>et al.</i> , 1998
Zn	FluoZin-3	C	Em. increase	100	510	Pancreatic B-cells	Gee <i>et al.</i> , 2002
413 nm laser activation	Photo-activatable GFP	G	Em. increase	100	520	Cos-7 cells	Patterson <i>et al.</i> , 2002
488 nm laser activation	Dendra	G	Em. increase	150	575	Hela cells	Gurskaya <i>et al.</i> , 2006

probes, however, have been successfully developed using a FRET pair of fluorescent proteins and carbohydrate binding linker (Fehr *et al.*, 2002).

Other recent advances in targeted imaging include a photoactivatable GFP mutant that only becomes fluorescent after shorter wavelength laser irradiation (Patterson *et al.*, 2002). By irradiating certain regions of the cell, the movement of tagged proteins from that area can be traced over time. This type of GFP has been used to image drosophila embryo *in vivo* (Post *et al.*, 2004). Furthermore, different variants have been developed that shift wavelength and are activatable with a longer wavelength irradiation (Gurskaya *et al.*, 2006). Another recent technique in monitoring protein interaction is bifluorescence complementation (Hu *et al.*, 2002). In this technique, two proteins are tagged with partial polypeptides from a fluorescent protein. If the tagged proteins move close together to interact, the nonfluorescent polypeptides fold into the correct structure and fluoresce. This technique overcomes the difficulty of conventional FRET in adjusting for different relative concentrations of acceptor and donor.

3.7. Comparison of different probes

Many diverse smart probes exist that have a wide range of activators and spectral properties. A comparison of some of the probes mentioned in this review is shown in Table 1. The “Type” column refers to whether the probe is genetically encoded (“G”) or chemically synthesized (“C”). It should be noted that in some cases, researchers obtained varying degrees of probe activation *in vivo* and *in vitro*, often with the *in vitro* activation demonstrating greater activation increase. Where possible, the *in vivo* fold change is reported. In some cases, the fold change and emission properties were estimated from graphs in figures. The original references should be consulted for more accurate information.

4. Conclusion

Numerous optical activatable smart probes have been developed in the past decade that can detect a wide range of targets. Many of these probes are suited for the *in vivo* imaging of physiological and pathogenic processes in small animals. The usefulness of activatable optical imaging will increase as imaging systems improve resolution and depth capability. Although current smart probes will continue to be used, new generations of activatable optical imaging agents will be developed and will display better contrast and selectivity.

Combining PDT with activatable smart probes is an intriguing therapeutic paradigm. Although this technique is in its infancy, it has already shown to be a successful treatment for xenograft tumours in mice. Many of the synthetic activatable smart probes that have been developed have the potential to be adapted to a photodynamic probe by substituting the fluorophore for a photosensitizing agent. Smart probes that can become activated in certain environments and kill target

cells when treated with light have the potential to treat diseases with unprecedented specificity.

Acknowledgements

J.F.L. is supported by Canadian Cancer Society Grant #018510 through the National Cancer Institute of Canada.

References

1. Bai, Y., Zhang, B., Xu, J., Duan, C., Dang, D., Liu, D. and Meng, Q. "Conformational switching fluorescent chemosensor for chloride anion," *New. J. Chem.* **29**, 777–779 (2005).
2. Belousov, V. V., Fradkov, A. F., Lukyanov, K. A., Staroverov, D. B., Shakhbazov, K. S., Terskikh, A. V. and Lukyanov, S. "Genetically encoded fluorescent indicator for intracellular hydrogen peroxide," *Nat. Methods* **3**, 281–286 (2006).
3. Blum, G., von Degenfeld, G., Merchant, M. J., Blau, H. M. and Bogoyo, M. "Non-invasive optical imaging of cysteine protease activity using fluorescently quenched activity-based probes," *Nat. Chem. Biol.* **3**, 668–677 (2007).
4. Bratu, D. P., Cha, B., Mhlanga, M. M., Kramer, F. R. and Tyagi, S. "Visualizing the distribution and transport of mRNAs in living cells," *Proc. Natl. Acad. Sci. USA* **100**, 13308–13313 (2003).
5. Chen, J., Stefflova, K., Niedre, M. J., Wilson, B. C., Chance, B., Glickson, J. D. and Zheng, G. "Protease-triggered photosensitizing beacon based on singlet oxygen quenching and activation," *J. Am. Chem. Soc.* **126**, 11450–11451 (2004).
6. Chudakov, D. M., Lukyanov, S. and Lukyanov, K. A. "Fluorescent proteins as a toolkit for in vivo imaging," *Trends Biotechnol.* **23**, 605–613 (2005).
7. Cui, Z., Zhang, Z., Zhang, X., Wen, J., Zhou, Y. and Xie, W. "Visualizing the dynamic behavior of poliovirus plus-strand RNA in living host cells," *Nucleic. Acids. Res.* **33**, 3245–3252 (2005).
8. Dong, M., Tepp, W. H., Johnson, E. A. and Chapman, E. R. "Using fluorescent sensors to detect botulinum neurotoxin activity in vitro and in living cells," *Proc. Natl. Acad. Sci. USA* **101**, 14701–14706 (2004).
9. Dunphy, I., Vinogradov, S. A. and Wilson, D. F. "Oxyphor R2 and G2: phosphors for measuring oxygen by oxygen-dependent quenching of phosphorescence," *Anal. Biochem.* **310**, 191–198 (2002).
10. Farber, S. A., Pack, M., Ho, S. Y., Johnson, I. D., Wagner, D. S., Dosch, R., Mullins, M. C., Hendrickson, H. S., Hendrickson, E. K. and Halpern, M. E. "Genetic analysis of digestive physiology using fluorescent phospholipid reporters," *Science* **292**, 1385–1388 (2001).
11. Fehr, M., Frommer, W. B. and Lalonde, S. "Visualization of maltose uptake in living yeast cells by fluorescent nanosensors," *Proc. Natl. Acad. Sci. USA* **99**, 9846–9851 (2002).
12. Flors, C., Fryer, M. J., Waring, J., Reeder, B., Bechtold, U., Mullineaux, P. M., Nonell, S., Wilson, M. T. and Baker, N. R. "Imaging the production of singlet oxygen in vivo using a new fluorescent sensor, Singlet Oxygen Sensor Green," *J. Exp. Bot.* **57**, 1725–1734 (2006).
13. Funovics, M., Weissleder, R. and Tung, C. "Protease sensors for bioimaging," *Anal. Bioanal. Chem.* **377**, 956–963 (2003).

14. Gee, K. R., Zhou, Z., Qian, W. and Kennedy, R. "Detection and imaging of zinc secretion from pancreatic beta-cells using a new fluorescent zinc indicator," *J. Am. Chem. Soc.* **124**, 776–778 (2002).
15. Giepmans, B. N. G., Adams, S. R., Ellisman, M. H. and Tsien, R. Y. "The fluorescent toolbox for assessing protein location and function," *Science* **312**, 217–224 (2006).
16. Godavarty, A., Sevick-Muraca, E. M. and Eppstein, M. J. "Three-dimensional fluorescence lifetime tomography," *Med. Phys.* **32**, 992–1000 (2005).
17. Goel, G., Kumar, A., Puniya, A. K., Chen, W. and Singh, K. "Molecular beacon: a multitask probe," *J. Appl. Microbiol.* **99**, 435–442 (2005).
18. Grynkiewicz, G., Poenie, M. and Tsien, R. Y. "A new generation of Ca²⁺ indicators with greatly improved fluorescence properties," *J. Biol. Chem.* **260**, 3440–3450 (1985).
19. Gurskaya, N. G., Verkhusha, V. V., Shcheglov, A. S., Staroverov, D. B., Chepurnykh, T. V., Fradkov, A. F., Lukyanov, S. and Lukyanov, K. A. "Engineering of a monomeric green-to-red photoactivatable fluorescent protein induced by blue light," *Nat. Biotechnol.* **24**, 461–465 (2006).
20. Hara, M., Bindokas, V., Lopez, J. P., Kaihara, K., Landa, L. R., Harbeck, M. and Roe, M. W. "Imaging endoplasmic reticulum calcium with a fluorescent biosensor in transgenic mice," *Am. J. Physiol. Cell Physiol.* **287**, C932–C938 (2004).
21. Hideg, E., Barta, C., Kálai, T., Vass, I., Hideg, K. and Asada, K. "Detection of singlet oxygen and superoxide with fluorescent sensors in leaves under stress by photoinhibition or UV radiation," *Plant Cell Physiol.* **43**, 1154–1164 (2002).
22. Hu, C., Chinenov, Y. and Kerppola, T. K. "Visualization of interactions among bZIP and Rel family proteins in living cells using bimolecular fluorescence complementation," *Mol. Cell* **9**, 789–798 (2002).
23. Jaffer, F. A., Kim, D., Quinti, L., Tung, C., Aikawa, E., Pande, A. N., Kohler, R. H., Shi, G., Libby, P. and Weissleder, R. "Optical visualization of cathepsin K activity in atherosclerosis with a novel, protease-activatable fluorescence sensor," *Circulation* **115**, 2292–2298 (2007).
24. Jiang, T., Olson, E. S., Nguyen, Q. T., Roy, M., Jennings, P. A. and Tsien, R. Y. "Tumor imaging by means of proteolytic activation of cell-penetrating peptides," *Proc. Natl. Acad. Sci. USA* **101**, 17867–17872 (2004).
25. Johnson, I. "Fluorescent probes for living cells," *Histochem. J.* **30**, 123–140 (1998).
26. Kay, A. R. "Evidence for chelatable zinc in the extracellular space of the hippocampus, but little evidence for synaptic release of Zn," *J. Neurosci.* **23**, 6847–6855 (2003).
27. Kim, Y., Choi, Y., Weissleder, R. and Tung, C. "Membrane permeable esterase-activated fluorescent imaging probe," *Bioorg. Med. Chem. Lett.* **17**, 5054–5057 (2007).
28. Kojima, H., Nakatsubo, N., Kikuchi, K., Kawahara, S., Kirino, Y., Nagoshi, H., Hirata, Y. and Nagano, T. "Detection and imaging of nitric oxide with novel fluorescent indicators: diaminofluoresceins," *Anal. Chem.* **70**, 2446–2453 (1998).
29. Kwon, J. Y., Jang, Y. J., Lee, Y. J., Kim, K. M., Seo, M. S., Nam, W. and Yoon, J. "A highly selective fluorescent chemosensor for Pb²⁺," *J. Am. Chem. Soc.* **127**, 10107–10111 (2005).
30. Lee, D., Khaja, S., Velasquez-Castano, J. C., Dasari, M., Sun, C., Petros, J., Taylor, W. R. and Murthy, N. "In vivo imaging of hydrogen peroxide with chemiluminescent nanoparticles," *Nat. Mater.* **6**, 765–769 (2007).
31. Lin, J., Zhang, Z., Yang, J., Zeng, S., Liu, B. and Luo, Q. "Real-time detection of caspase-2 activation in a single living HeLa cell during cisplatin-induced apoptosis," *J. Biomed. Opt.* **11**, 024011 (2006).
32. Lin, Z., Xie, L., Zhao, Y., Duan, C. and Qu, J. "Thiourea-based molecular clips for fluorescent discrimination of isomeric dicarboxylates," *Org. Biomol. Chem.* **5**, 3535–3538 (2007).

33. Liu, L., Yermolaieva, O., Johnson, W. A., Abboud, F. M. and Welsh, M. J. "Identification and function of thermosensory neurons in *Drosophila* larvae," *Nat. Neurosci.* **6**, 267–273 (2003).
34. Lu, J., Zhang, Z., Yang, J., Chu, J., Li, P., Zeng, S. and Luo, Q. "Visualization of beta-secretase cleavage in living cells using a genetically encoded surface-displayed FRET probe," *Biochem. Biophys. Res. Commun.* **362**, 25–30 (2007).
35. Mahmood, U., Tung, C. H., Bogdanov, A. and Weissleder, R. "Near-infrared optical imaging of protease activity for tumor detection," *Radiology* **213**, 866–870 (1999).
36. Massoud, T. F. and Gambhir, S. S. "Molecular imaging in living subjects: seeing fundamental biological processes in a new light," *Genes. Dev.* **17**, 545–580 (2003).
37. McIntyre, J. O., Fingleton, B., Wells, K. S., Piston, D. W., Lynch, C. C., Gautam, S. and Matrisian, L. M. "Development of a novel fluorogenic proteolytic beacon for in vivo detection and imaging of tumour-associated matrix metalloproteinase-7 activity," *Biochem. J.* **377**, 617–628 (2004).
38. Meade, T. J., Taylor, A. K. and Bull, S. R. "New magnetic resonance contrast agents as biochemical reporters," *Curr. Opin. Neurobiol.* **13**, 597–602 (2003).
39. Miesenböck, G., Angelis, D. A. D. and Rothman, J. E. "Visualizing secretion and synaptic transmission with pH-sensitive green fluorescent proteins," *Nature* **394**, 192–195 (1998).
40. Miller, E. W., Tulyathan, O., Tulyanthan, O., Isacoff, E. Y. and Chang, C. J. "Molecular imaging of hydrogen peroxide produced for cell signaling," *Nat. Chem. Biol.* **3**, 263–267 (2007).
41. Mitra, R. D., Silva, C. M. and Youvan, D. C. "Fluorescence resonance energy transfer between blue-emitting and red-shifted excitation derivatives of the green fluorescent protein," *Gene* **173**, 13–17 (1996).
42. Miyawaki, A., Llopis, J., Heim, R., McCaffery, J. M., Adams, J. A., Ikura, M. and Tsien, R. Y. "Fluorescent indicators for Ca²⁺ based on green fluorescent proteins and calmodulin," *Nature* **388**, 882–887 (1997).
43. Moerner, W. E. "New directions in single-molecule imaging and analysis," *Proc. Natl. Acad. Sci. USA* **104**, 12596–12602 (2007).
44. Molenaar, C., Marras, S. A., Slat, J. C., Truffert, J. C., Lemaître, M., Raap, A. K., Dirks, R. W. and Tanke, H. J. "Linear 2' O-Methyl RNA probes for the visualization of RNA in living cells," *Nucleic Acids Res.* **29**, E89–E89 (2001).
45. Moschou, E. A., Sharma, B. V., Deo, S. K. and Daunert, S. "Fluorescence glucose detection: advances toward the ideal in vivo biosensor," *J. Fluoresc.* **14**, 535–547 (2004).
46. Nesterov, E. E., Skoch, J., Hyman, B. T., Klunk, W. E., Bacskai, B. J. and Swager, T. M. "In vivo optical imaging of amyloid aggregates in brain: design of fluorescent markers," *Angew. Chem. Int. Ed. Engl.* **44**, 5452–5456 (2005).
47. Ntziachristos, V., Tung, C., Bremer, C. and Weissleder, R. "Fluorescence molecular tomography resolves protease activity in vivo," *Nat. Med.* **8**, 757–760 (2002).
48. Ntziachristos, V., Yodh, A. G., Schnall, M. and Chance, B. "Concurrent MRI and diffuse optical tomography of breast after indocyanine green enhancement," *Proc. Natl. Acad. Sci. USA* **97**, 2767–2772 (2000).
49. O'Riordan, T. C., Fitzgerald, K., Ponomarev, G. V., Mackrill, J., Hynes, J., Taylor, C. and Papkovsky, D. B. "Sensing intracellular oxygen using near-infrared phosphorescent probes and live-cell fluorescence imaging," *Am. J. Physiol. Regul. Integr. Comp. Physiol.* **292**, R1613–R1620 (2007).
50. Oleinick, N. L. and Evans, H. H. "The photobiology of photodynamic therapy: cellular targets and mechanisms," *Radiat. Res.* **150**, S146–S156 (1998).

51. Patterson, G. H. and Lippincott-Schwartz, J. "A photoactivatable GFP for selective photolabeling of proteins and cells," *Science* **297**, 1873–1877 (2002).
52. Peter, M. and Ameer-Beg, S. M. "Imaging molecular interactions by multiphoton FLIM," *Biol. Cell* **96**, 231–236 (2004).
53. Petrat, F., Weisheit, D., Lensen, M., de Groot, H., Sustmann, R. and Rauen, U. "Selective determination of mitochondrial chelatable iron in viable cells with a new fluorescent sensor," *Biochem. J.* **362**, 137–147 (2002).
54. Post, J. N., Lidke, K. A., Rieger, B. and Arndt-Jovin, D. J. "One- and two-photon photoactivation of a paGFP-fusion protein in live *Drosophila* embryos," *FEBS Lett.* **579**, 325–330 (2005).
55. Ramanujan, V. K., Zhang, J., Biener, E. and Herman, B. "Multiphoton fluorescence lifetime contrast in deep tissue imaging: prospects in redox imaging and disease diagnosis," *J. Biomed. Opt.* **10**, 051407 (2005).
56. Richards-Kortum, R. and Sevick-Muraca, E. "Quantitative optical spectroscopy for tissue diagnosis," *Annu. Rev. Phys. Chem.* **47**, 555–606 (1996).
57. Russell, J., Diamond, K., Collins, T., Weston M., Lovell J., Hayward, J., Farrell, T., Patterson, M. and Fang, Q. "Characterization of time-domain fluorescence properties of typical photosensitizers for photodynamic therapy," *Proc. SPIE* **6437**, 64270G1-9 (2007).
58. Sando, S., Abe, H. and Kool, E. T. "Quenched auto-ligating DNAs: multicolor identification of nucleic acids at single nucleotide resolution," *J. Am. Chem. Soc.* **126**, 1081–1087 (2004).
59. Santangelo, P. J., Nix, B., Tsourkas, A. and Bao, G. "Dual FRET molecular beacons for mRNA detection in living cells," *Nucleic. Acids. Res.* **32**, e57 (2004).
60. Skala, M. C., Ricking, K. M., Bird, D. K., Gendron-Fitzpatrick, A., Eickhoff, J., Eliceiri, K. W., Keely, P. J. and Ramanujam, N. "In vivo multiphoton fluorescence lifetime imaging of protein-bound and free nicotinamide adenine dinucleotide in normal and precancerous epithelia," *J. Biomed. Opt.* **12**, 024014 (2007).
61. Stefflova, K., Chen, J. and Zheng, G. "Killer beacons for combined cancer imaging and therapy," *Curr. Med. Chem.* **14**, 2110–2125 (2007).
62. Stefflova, K., Chen, J. and Zheng, G. "Using molecular beacons for cancer imaging and treatment," *Frontiers in Bioscience* **12**, 4709–4721 (2007).
63. Tan, W., Wang, K. and Drake, T. J. "Molecular beacons," *Curr. Opin. Chem. Biol.* **8**, 547–553 (2004).
64. Truong, K., Sawano, A., Mizuno, H., Hama, H., Tong, K., Mal, T., Miyawaki, A. and Ikura, M. "FRET-based in vivo Ca²⁺ imaging by a new calmodulin-GFP fusion molecule," *Nat. Struct. Biol.* **8**, 1069–1073 (2001).
65. Tung, C., Zeng, Q., Shah, K., Kim, D., Schellingerhout, D. and Weissleder, R. "In vivo imaging of beta-galactosidase activity using far red fluorescent switch," *Cancer Res.* **64**, 1579–1583 (2004).
66. Tyagi, S. and Kramer, F. R. "Molecular beacons: probes that fluoresce upon hybridization," *Nat. Biotechnol.* **14**, 303–308 (1996).
67. Vargas, D. Y., Raj, A., Marras, S. A. E., Kramer, F. R. and Tyagi, S. "Mechanism of mRNA transport in the nucleus," *Proc. Natl. Acad. Sci. USA* **102**, 17008–17013 (2005).
68. Wehrman, T. S., von Degenfeld, G., Krutzik, P. O., Nolan, G. P. and Blau, H. M. "Luminescent imaging of beta-galactosidase activity in living subjects using sequential reporter-enzyme luminescence," *Nat. Methods* **3**, 295–301 (2006).
69. Weissleder, R., Tung, C. H., Mahmood, U. and Bogdanov, A. "In vivo imaging of tumors with protease-activated near-infrared fluorescent probes," *Nat. Biotechnol.* **17**, 375–378 (1999).

70. Xi, C., Balberg, M., Boppart, S. A. and Raskin, L. "Use of DNA and peptide nucleic acid molecular beacons for detection and quantification of rRNA in solution and in whole cells," *Appl. Environ. Microbiol.* **69**, 5673–5678 (2003).
71. Yang, L., McRae, R., Henary, M. M., Patel, R., Lai, B., Vogt, S. and Fahrni, C. J. "Imaging of the intracellular topography of copper with a fluorescent sensor and by synchrotron x-ray fluorescence microscopy," *Proc. Natl. Acad. Sci. USA* **102**, 11179–11184 (2005).
72. Yasui, H. and Sakurai, H. "Chemiluminescent detection and imaging of reactive oxygen species in live mouse skin exposed to UVA," *Biochem. Biophys. Res. Commun.* **269**, 131–136 (2000).
73. Zhang, J., Ma, Y., Taylor, S. S. and Tsien, R. Y. "Genetically encoded reporters of protein kinase A activity reveal impact of substrate tethering," *Proc. Natl. Acad. Sci. USA* **98**, 14997–15002 (2001).
74. Zhang, Z., Yang, J., Lu, J., Lin, J., Zeng, S. and Luo, Q. "Fluorescence imaging to assess the matrix metalloproteinase activity and its inhibitor in vivo," *J. Biomed. Opt.* **13**, 011006 (2008).
75. Zheng, G., Chen, J., Stefflova, K., Jarvi, M., Li, H. and Wilson, B. C. "Photodynamic molecular beacon as an activatable photosensitizer based on protease-controlled singlet oxygen quenching and activation," *Proc. Natl. Acad. Sci. USA* **104**, 8989–8994 (2007).
76. Zipfel, W. R., Williams, R. M. and Webb, W. W. "Nonlinear magic: multiphoton microscopy in the biosciences," *Nat. Biotechnol.* **21**, 1369–1377 (2003).